Received: 9 July 2020 | Revised: 21 August 2020 | Accepted: 26 August 2020

DOI: 10.1002/ardp.202000235

FULL PAPER

ARCH PHARM DPhG
Archiv der Pharmazie

A new series of benzoxazole-based SIRT1 modulators for targeted therapy of non-small-cell lung cancer

Belgin Sever[1] | Gülşen Akalın Çiftçi[2] | Mehlika Dilek Altıntop[1]

[1]Department of Pharmaceutical Chemistry, Faculty of Pharmacy, Anadolu University, Eskişehir, Turkey

[2]Department of Biochemistry, Faculty of Pharmacy, Anadolu University, Eskişehir, Turkey

Correspondence
Belgin Sever, Department of Pharmaceutical Chemistry, Faculty of Pharmacy, Anadolu University, 26470 Eskişehir, Turkey.
Email: belginsever@anadolu.edu.tr

Abstract

In an attempt to identify potential anticancer agents for non-small-cell lung cancer (NSCLC) targeting sirtuin 1 (SIRT1), the synthesis of a new series of benzoxazoles (**3a** – **i**) was carried out through a facile and versatile synthetic route. The compounds were evaluated for their cytotoxic effects on A549 human lung adenocarcinoma and NIH/3T3 mouse embryonic fibroblast cells using the MTT assay. 2-[(5-Nitro-1*H*-benzimidazol-2-yl)thio]-*N*-(2-methylbenzoxazol-5-yl)acetamide (**3e**) and 2-[(5-chloro-1*H*-benzimidazol-2-yl)thio]-*N*-(2-methylbenzoxazol-5-yl)acetamide (**3g**) were the most potent and selective anticancer agents in this series against the A549 cell line, with IC_{50} values of 46.66 ± 11.54 and 55.00 ± 5.00 μM, respectively. The flow cytometry-based apoptosis detection assay was performed to determine their effects on apoptosis in A549 cells. Both compounds induced apoptosis in a dose-dependent manner. The effects of compounds **3e** and **3g** on SIRT1 activity were determined. On the basis of in vitro studies, it was observed that compound **3g** caused a significant decrease in SIRT1 levels in a dose-dependent manner, whereas compound **3e** increased the SIRT1 levels. According to molecular docking studies, the substantial alteration in the type of action could be attributed to the difference between the interactions of compounds **3e** and **3g** with the same residues in the active site of SIRT1 (PDB code: 4IG9). On the basis of in silico ADME (absorption, distribution, metabolism, and excretion) studies, these compounds are predicted to possess favorable ADME profiles. According to the in vitro and in silico studies, compounds **3e** and **3g**, small-molecule SIRT1 modulators, were identified as potential orally bioavailable anticancer agents for the targeted therapy of NSCLC.

KEYWORDS

apoptosis, benzimidazole, benzoxazole, molecular docking, non-small-cell lung cancer, SIRT1

1 | INTRODUCTION

Non-small-cell lung cancer (NSCLC), which accounts for almost 85% of lung cancer (LC) cases, remains the leading cause of cancer-related mortality across the globe, with rates increasing in the past decade. Despite recent advances in diagnosis and combined treatments including surgical resection, radiotherapy, and chemotherapy, the overall survival for NSCLC patients still remains poor. Surgical resection is still the best option for the treatment of NSCLC, but most patients are diagnosed at advanced or metastatic stages (Stage III/IV) when surgery is no longer a therapeutic option; therefore, chemotherapy and radiotherapy gain prominence as important therapeutic approaches for unresectable NSCLC. Platinum-based chemotherapeutic drugs often cause severe side effects, as these agents destroy healthy cells as well as tumor cells. As a consequence, targeted therapies acting on specific molecular targets have emerged as promising therapeutic options for NSCLC to improve therapeutic efficacy and overcome toxicity problems.[1-5]

Sirtuins (SIRTs), NAD^+-dependent class III histone deacetylases, have emerged as potential therapeutic targets due to their crucial roles in diverse physiological and pathological processes such as gene transcription, energy metabolism, lipid metabolism, insulin secretion, lifespan extension, neurodegeneration, age-related disorders, obesity, heart disease, inflammation, and cancer.[6,7] In mammals, there are seven members (SIRT1–SIRT7) in the sirtuin family. In particular, SIRT1 has been the most extensively studied member of this family. In recent years, the dual role of SIRT1 in cancer has become a highly controversial topic. SIRT1 acts as either a tumor suppressor or as an oncogenic factor, depending on the cellular context or its targets in specific signaling pathways or specific cancers. The modulation of SIRT1 activity by small-molecule activators or inhibitors stands out as a promising strategy for the management of many types of cancer including NSCLC.[7-13]

Heterocycles are common fragments of the vast majority of marketed drugs. This is a reflection of their pivotal role in drug discovery and development.[14,15] Among heterocycles, benzoxazoles occupy a prominent place in contemporary medicinal chemistry as building blocks for modulating affinity and/or selectivity of a ligand toward a particular target through favorable interactions such as hydrogen bonds, cation–π, π–π stacking, and hydrophobic interactions; thus, the benzoxazole core is found in ligands targeting a plethora of receptors and enzymes involved in the pathogenesis of many diseases including cancer. Due to their important features, benzoxazole derivatives are suitable candidates for targeted therapy of cancer.[16-25] Besides, benzimidazole is a hot topic of research in pharmaceutical industry as a privileged scaffold due to its diverse therapeutic applications associated with its ability to bind with a variety of enzymes and receptors *via* proper interactions such as hydrogen bonds, ion–dipole, cation–π, π–π stacking, hydrophobic effect, the van der Waals force, and so on.[26-36] Benzimidazole is a structural isostere of indole and purine nuclei, and this core is also an integral part of the structure of vitamin B_{12}. In particular, benzimidazoles exhibit potent antitumor activity against various cancer cell lines through different mechanisms including the inhibition of several crucial targets such as epidermal growth factor receptor, vascular endothelial growth factor receptor, platelet-derived growth factor receptor, cyclin-dependent kinases, aurora kinases, mitogen-activated protein kinases, polo-like kinases, casein kinases, checkpoint kinases, and sirtuins.[26-35]

On the basis of the aforementioned findings, herein we described the design and synthesis of a new series of benzoxazoles as potential anticancer agents for targeted therapy of NSCLC and carried out in silico and in vitro studies to elucidate their mode of action.

2 | RESULTS AND DISCUSSION

2.1 | Chemistry

The facile and efficient synthetic route for the preparation of the hitherto unreported benzoxazoles (**3a – i**) is depicted in Scheme 1.

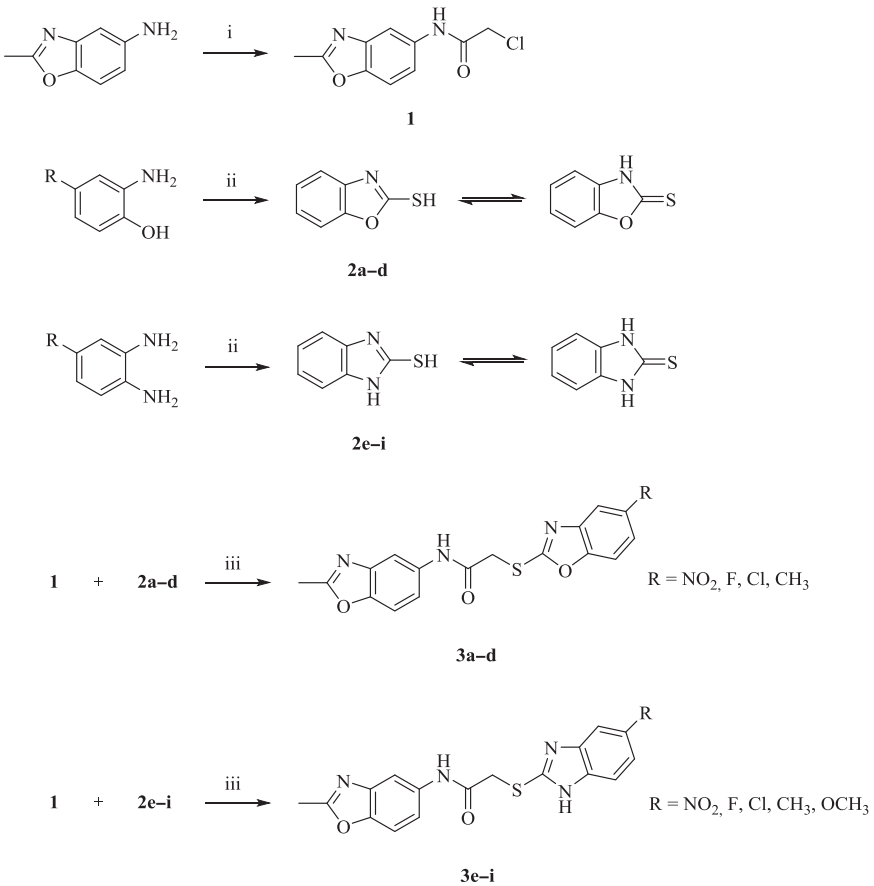

SCHEME 1 The synthetic route for the preparation of compounds **3a–i**. Reagents and conditions: (i) $ClCOCH_2Cl$, TEA, toluene, rt; (ii) (1) CS_2, KOH, ethanol, reflux, 8 hr, (2) CH_3COOH; (iii) K_2CO_3, acetone, rt, 12 hr. rt, room temperature

TABLE 1 IC_{50} values of the compounds against A549 and NIH/3T3 cells for 24 hr

Compound	IC_{50} (μM)		SI[a]
	A549 cell line	NIH/3T3 cell line	
3a	350.00 ± 70.71	>500	>1.43
3b	>500	>500	ND
3c	253.33 ± 87.37	>500	>1.97
3d	>500	>500	ND
3e	46.66 ± 11.54	383.33 ± 5.77	8.22
3f	230.00 ± 26.46	440.00 ± 52.92	1.91
3g	55.00 ± 5.00	>500	>9.09
3h	>500	>500	ND
3i	>500	>500	ND
Cisplatin	27.00 ± 1.73	ND	ND

Abbreviations: ND, not determined, SI, selectivity index.
[a]SI = IC_{50} for NIH/3T3 cells/IC_{50} for A549 cells.

Initially, 2-chloro-*N*-(2-methylbenzoxazol-5-yl)acetamide (**1**) was synthesized *via* the reaction of 5-amino-2-methylbenzoxazole with chloroacetyl chloride in the presence of triethylamine (TEA). However, the ring closure reaction of 4-substituted-*o*-aminophenol derivatives (**2a** – **d**) with carbon disulfide in the presence of potassium hydroxide yielded 5-substituted benzoxazole-2-thiol derivatives (**3a** – **d**) (Scheme 1). Similarly, the ring closure reaction of 4-substituted-*o*-phenylenediamine derivatives (**2e** – **i**) with carbon disulfide in the presence of potassium hydroxide afforded 5-substituted 1*H*-benzimidazole-2-thiol derivatives (**3e** – **i**). Finally, compounds **2a** – **i** were reacted with compound **1** in the presence of potassium carbonate to afford compounds **3a – i**.

The structures of compounds **3a – i** were verified by different spectroscopic techniques, namely ınfrared (IR), ^{1}H nuclear magnetic resonance (NMR), ^{13}C NMR, and high-resolution mass spectrometry (HRMS). In the IR spectra of compounds **3a – i**, the C═O stretching vibration led to the formation of the characteristic amide I band at 1,675.15–1,660.71 cm^{-1}. The N-H stretching vibrations belonging to the secondary amide group gave rise to the bands in the region 3,336.85–3,269.34 cm^{-1}. Aromatic and aliphatic C—H stretching bands occurred at 3,134.33–3,001.24 cm^{-1} and 2,983.88–2,808.36 cm^{-1}, respectively. The N—H bending, C═N, and C═C stretching bands appeared between 1,633.71 and 1,456.26 cm^{-1}. In their ^{1}H NMR spectra, the signal due to the amide N—H proton appeared at 10.60–10.76 ppm as a singlet. The S—CH_2 protons gave rise to a singlet peak at 4.20–4.42 ppm. The signals due to the methyl protons at the 2nd position of the benzoxazole scaffold appeared at 2.60–2.65 ppm. The signals due to the heteroaromatic protons were observed in the region 6.74–8.33 ppm. In the ^{1}H NMR spectra of compounds **3e** – **i**, the signal due to the N—H proton of the benzimidazole core appeared at 12.56–12.87 ppm as a broad singlet. In their ^{13}C NMR spectra, the signal due to the amide C═O carbon was observed at 165.58–171.89 ppm. The S—CH_2 carbon gave rise to a peak in the region 32.81–37.71 ppm. The signal due to the methyl carbon at the 2nd position of the benzoxazole ring appeared at 14.09–14.13 ppm. The HRMS data of all compounds were consistent with their proposed structures.

2.2 | In vitro anticancer activity

The MTT assay, a tetrazolium-based colorimetric assay, was performed to assess the cytotoxic effects of compounds **3a – i** on the A549 human lung adenocarcinoma cell line (Table 1). In order to evaluate whether these compounds were toxic or nontoxic to normal cells, their cytotoxic effects on NIH/3T3 mouse embryonic fibroblast (normal) cells were investigated, and their selectivity index (SI) values are presented in Table 1. Compounds **3a** – **d** bearing two benzoxazole moieties did not show any significant cytotoxic activity against A549 cells. In general, the replacement of the benzoxazole scaffold of compounds **3a** and **3c** with the benzimidazole scaffold of compounds **3e** and **3g** led to a significant increase in potency. Compounds **3e** and **3g** exhibited a marked cytotoxic activity against the A549 cells, with IC_{50} values of 46.66 ± 11.54 and 55.0 ± 5.0 μM, respectively, as compared with cisplatin (IC_{50} = 27.0 ± 1.73 μM). Additionally, the SI values of compounds **3e** and **3g** were determined as 8.22 and >9.09, respectively, indicating that their anticancer effects on A549 cells were selective. The results pointed out the importance of the

TABLE 2 Percentages of typical quadrant analysis of Annexin V-FITC/PI flow cytometry of A549 cells treated with compounds **3e**, **3g**, and cisplatin

Groups	Early apoptotic cells (%)	Late apoptotic cells (%)	Viable cells (%)	Necrotic cells (%)
Control (untreated)	5.1	6.1	82.8	5.9
Cells treated with IC_{50}/2 concentration of compound **3e**	9.0	18.2	57.4	15.4
Cells treated with IC_{50} concentration of compound **3e**	20.4	28.7	32.7	18.0
Cells treated with IC_{50}/2 concentration of compound **3g**	11.6	22.0	55.8	10.6
Cells treated with IC_{50} concentration of compound **3g**	20.4	45.7	24.7	8.6
Cells treated with IC_{50} concentration of cisplatin	11.9	41.0	29.1	18.0

Note: A549 cells were cultured for 24 hr in a medium with IC_{50}/2 and IC_{50} concentrations of compounds **3e** and **3g** and IC_{50} concentration of cisplatin. At least 10,000 cells were analyzed per sample, and quadrant analysis was performed.

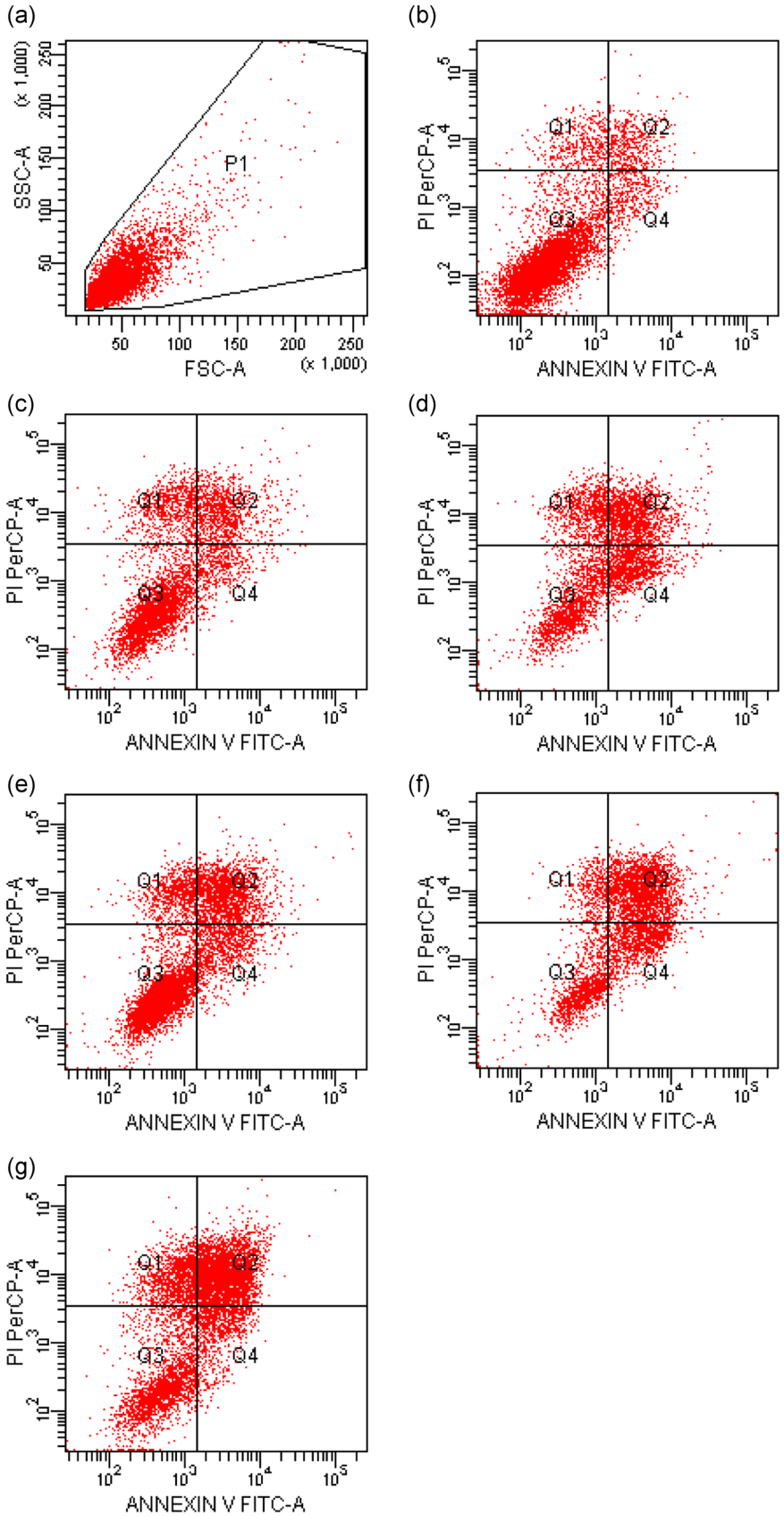

FIGURE 1 A typical quadrant analysis of Annexin V-FITC/PI flow cytometric analysis of A549 cells treated with different concentrations of compounds **3e**, **3g**, and cisplatin. At least 10,000 cells were analyzed per sample, and quadrant analysis was performed. Q1, Q2, Q3, and Q4 quadrants represent necrosis, late apoptosis, viable cells, and early apoptotic cells, respectively. A549 cells were cultured for 24 hr in a medium with $IC_{50}/2$ and IC_{50} concentrations of the compounds. (a,b) Untreated control cells. (c,d) Cells treated with $IC_{50}/2$ and IC_{50} concentrations of compound **3e**. (e,f) Cells treated with $IC_{50}/2$ and IC_{50} concentrations of compound **3g**. (g) Cells treated with IC_{50} concentration of cisplatin, respectively

TABLE 3 The effects of compounds **3e**, **3g**, and cisplatin on SIRT1 activity

Compound	SIRT1 concentration (ng/ml)
Control	3.12 ± 0.03
3e (23.33 μM)	4.53 ± 1.26
3e (46.66 μM)	3.67 ± 1.03
3g (27.5 μM)	2.10 ± 0.35
3g (55 μM)	1.31 ± 0.04
Cisplatin (13.5 μM)	4.53 ± 1.37
Cisplatin (27 μM)	3.32 ± 1.41

benzimidazole core as well as the substituent at position 5 of the benzimidazole ring for anticancer activity against A549 cells. The nitro and chloro substituents at the 5-position of the benzimidazole ring enhanced the cytotoxic activity against the A549 cell line.

Apoptosis is a physiological process that is essential for the removal of damaged or redundant cells and maintenance of cellular homeostasis. However, in cancerogenesis, deregulated apoptotic signaling, particularly the activation of antiapoptotic systems, allows cancer cells to escape from this crucial process, leading to uncontrolled proliferation, which further results in tumor survival, therapeutic resistance, and recurrence of cancer. Mounting evidence has revealed that many anticancer agents induce apoptosis and related cell death networks to eliminate tumor cells, and thus the induction of apoptosis is of great importance for the management of many types of cancer including NSCLC.[37-41] In order to identify early and late apoptotic cells, after 24-hr incubation of A549 cells treated with compounds **3e** and **3g** at $IC_{50}/2$ and IC_{50} concentrations and cisplatin at IC_{50} concentration, the flow cytometry-based apoptosis detection assay was performed by means of Annexin V-fluorescein isothiocyanate (FITC)/propidium iodide (PI) staining. The percentages of A549 cells undergoing early apoptosis exposed to compounds **3e** and **3g** at $IC_{50}/2$ and IC_{50} concentrations were found to be 9.0%, 20.4%, 11.6%, and 20.4%, respectively. The percentages of A549 cells undergoing late apoptosis exposed to compounds **3e** and **3g** at $IC_{50}/2$ and IC_{50} concentrations were determined as 18.2%, 28.7%, 22.0%, and 45.7%, respectively (Table 2 and Figure 1). However, the percentages of A549 cells undergoing early and late apoptosis exposed to cisplatin were found as 11.9% and 41%, respectively. According to these findings, both compounds induced apoptosis in a dose-dependent manner. In particular, compound **3g** caused a more significant apoptotic activity than compound **3e** and cisplatin at IC_{50} concentration.

In an effort to provide insights into the mechanism underlying their cytotoxic and apoptotic effects on NSCLC, the effects of compounds **3e** and **3g** at $IC_{50}/2$ and IC_{50} concentrations on SIRT1 activity in the C6 rat glioma cell line were investigated using the enzyme-linked Immunosorbent assay (ELISA)-based assay (Table 3 and Figure 2). According to the assay, compound **3g** decreased SIRT1 levels in a dose-dependent manner at 27.5 and 55 μM concentrations. The SIRT1 activity inhibition value for compound **3g** at $IC_{50}/2$ concentration was found as 32.70%, whereas the SIRT1 activity inhibition value for compound **3g** at IC_{50} concentration was determined as 60.66%. However, compound **3e** increased SIRT1 levels in the C6 rat glioma cell line at 23.33 and 46.66 μM, similar to cisplatin. It can be concluded that these compounds exhibit their anticancer activity through different mechanisms of action. Compound **3g** acts as a SIRT1 inhibitor, whereas compound **3e** acts as a SIRT1 activator. According to these results, the chloro substitution at the 5-position of the benzimidazole scaffold led to SIRT1 inhibition, whereas the nitro substitution at position 5 of the benzimidazole ring resulted in SIRT1 activation. Taking into account the fact that SIRT1 acts as a double-edged sword in cancer,[7-13] both agents could be beneficial for the management of cancer.

2.3 | Molecular docking studies

Molecular docking studies were performed to elucidate the possible binding modes of compound **3e** (SIRT1 activator) and compound **3g** (SIRT1 inhibitor) in the active site of SIRT1 (PDB code: 4IG9) using

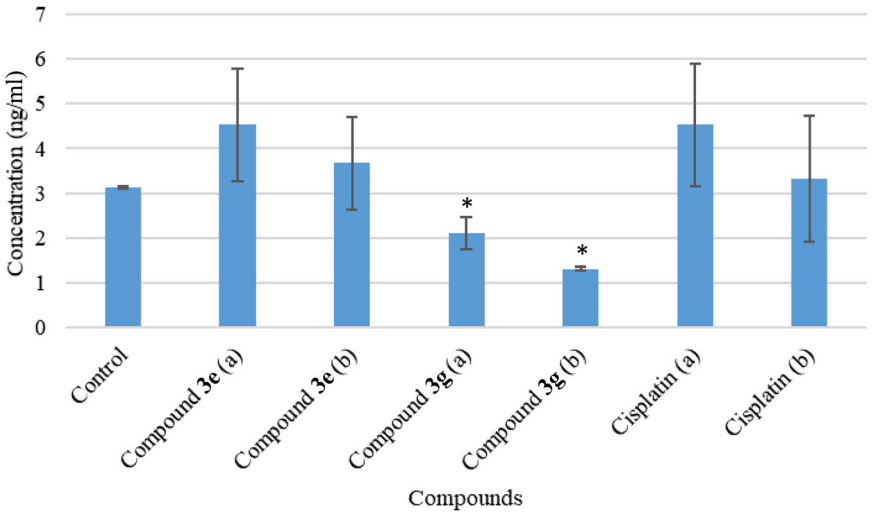

FIGURE 2 The effects of compounds **3e** (a: 23.33 μM, b: 46.66 μM), **3g** (a: 27.5 μM, b: 55 μM), and cisplatin (a: 13.5 μM, b: 27 μM) on SIRT1 levels in the C6 rat glioma cell line. *Significance from control group $p < .05$

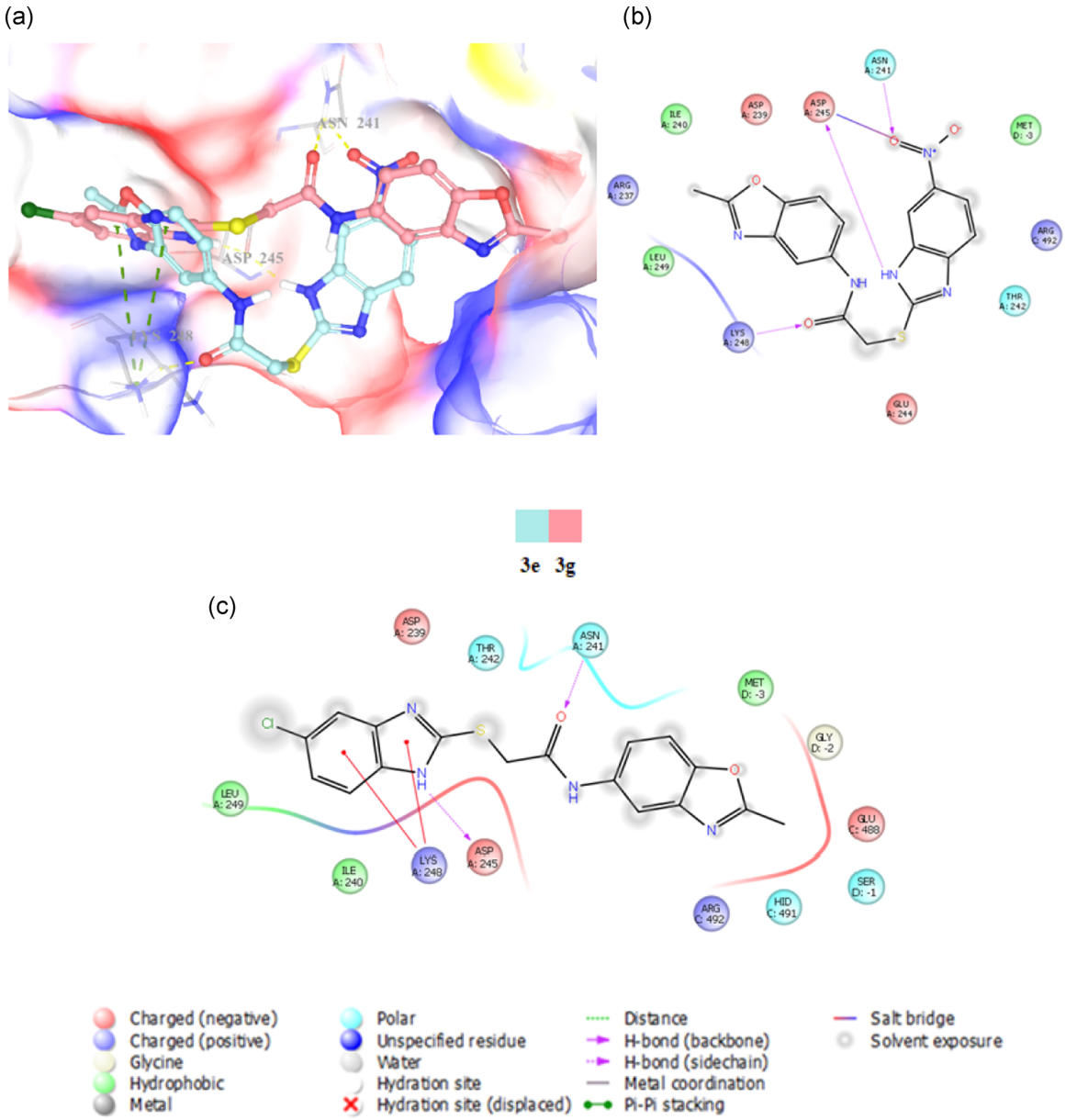

FIGURE 3 Docking poses (a) and interactions of compounds **3e** (b) and **3g** (c) in the active site of SIRT1 (PDB code: 4IG9)

Schrödinger's Maestro molecular modeling package. Molecular docking studies indicated that compounds **3e** and **3g** showed high affinity in the active site of SIRT1, as depicted in Figure 3. In the active site of SIRT1, compound **3e** was capable of forming hydrogen bonds with Lys248 and Asp245 residues due to the presence of the amide carbonyl group and the benzimidazole N—H moiety. The nitro substituent at position 5 of the benzimidazole scaffold formed a hydrogen bond with Asn241 and a salt bridge with Asp245. However, compound **3g** was capable of forming hydrogen bonds with Asn241 and Asp245 residues due to the presence of the amide carbonyl group and the benzimidazole N—H moiety. The benzimidazole moiety carrying a chloro substituent at the 5-position formed cation–π interactions with the Lys248 residue. In silico studies suggested that the difference between the interactions of compounds **3e** and **3g** with the same residues in the active site of SIRT1 might be responsible for the substantial alteration in the type of action (inhibition or activation).

2.4 | In silico absorption, distribution, metabolism, and excretion (ADME) studies

The pharmacokinetic profiles of compounds **3a** – **i** were predicted by means of QikProp, a predictive ADME module within the Maestro suite produced by Schrödinger (Table 4). According to in silico prediction, the total solvent-accessible surface area (SASA), the predicted octanol/water partition coefficient (QPlogPo/w), the conformation-independent predicted aqueous solubility (CIQPlogS), and the

TABLE 4 Predicted ADME profiles of compounds **3a–i**

Compound	SASA[a]	QPlogPo/w[a]	ClQPlogS[a]	QPlogKhsa[a]	Human oral absorption %[b]	Rule of five[c]	Rule of three[c]
3a	647.916	2.262	−5.109	−0.078	80.215	0	0
3b	617.976	3.203	−4.966	0.020	100.000	0	0
3c	632.953	3.457	−5.296	0.090	100.000	0	0
3d	641.093	3.272	−4.887	0.130	100.000	0	0
3e	663.637	2.302	−5.268	0.072	76.364	0	0
3f	635.540	3.235	−5.109	0.153	100.000	0	0
3g	648.794	3.473	−5.433	0.218	100.000	0	0
3h	658.002	3.293	−5.032	0.259	100.000	0	0
3i	663.517	3.100	−5.068	0.126	100.000	0	0

[a]Recommended values for SASA: 300–1,000 Å^2; QPlogPo/w: −2 to 6.5; ClQPlogS: −6.5 to 0.5; QPlogKhsa: −1.5 to 1.5.
[b]Predicted human oral absorption on 0–100% scale. Human oral absorption higher than 80% is considered to be high, whilst human oral absorption lower than 25% is considered to be poor.
[c]Number of violations of Lipinski's rule of five. The rules are molecular weight of the molecule < 500, QPlogPo/w < 5, hydrogen-bond donor atoms ≤ 5, hydrogen-bond acceptor atoms ≤ 10. Compounds that obey these rules are considered as drug-like molecules. Rule of three: Number of violations of Jorgensen's rule of three. The three rules are QPlogS (predicted aqueous solubility) > −5.7, QPPCaco > 22 nm/s, #Primary Metabolites < 7. Compounds with fewer (and preferably no) violations of these rules are more likely to be orally available agents (Schrödinger Release 2016-2; Schrödinger, LLC, New York, NY).

predicted binding to human serum albumin (QPlogKhsa) values of all compounds were within the optimum range. The human oral absorption percentages of the compounds were found to be in the range of 76.364–100.000%. All compounds comply with Lipinski's rule of five and Jorgensen's rule of three. On the basis of these results, they are expected to possess favorable oral bioavailability and drug-like properties.

3 | CONCLUSIONS

In this paper, the synthesis of a new series of benzoxazoles was carried out according to a facile and versatile synthetic procedure. All compounds were evaluated for their cytotoxic effects on A549 and NIH/3T3 cells. Compounds **3e** and **3g** were identified as the most potent and selective anticancer agents against A549 cell line in this series. These agents were also evaluated for their effects on apoptosis in the A549 cell line. The findings demonstrated that A549 cells treated with both compounds underwent apoptosis. In particular, compound **3g** showed a more significant apoptotic activity than compound **3e** and cisplatin. In an attempt to elucidate their mechanism of action, the effects of compounds **3e** and **3g** at $IC_{50}/2$ and IC_{50} concentrations on SIRT1 activity in the C6 rat glioma cell line were investigated. Compound **3g** significantly inhibited SIRT1 in a dose-dependent manner, whereas compound **3e** caused an increase in SIRT1 levels. According to molecular docking studies, the difference between the interactions of compounds **3e** and **3g** with the same residues in the active site of SIRT1 (PDB code: 4IG9) might be responsible for the considerable alteration in the type of action (inhibition or activation). On the basis of in silico ADME studies, these compounds are expected to possess favorable ADME profiles. According to in vitro and in silico studies, compounds **3e** and **3g**, small-molecule SIRT1 modulators in this series, stand out as potential orally bioavailable anticancer agents for targeted therapy of NSCLC. In the continuation of this study, further studies are needed to provide insights into the mechanism underlying the alteration in their type of action (SIRT1 inhibition or activation).

4 | EXPERIMENTAL

4.1 | Chemistry

4.1.1 | General

The chemicals used in this study were procured from Acros Organics (Geel, Belgium), Sigma-Aldrich (St. Louis, MO), or Merck (Darmstadt, Germany), and they were used without further purification. The melting points (m.p.) of the synthesized compounds were determined by an MP90 digital melting point apparatus (Mettler Toledo, OH) and were uncorrected. IR spectra were recorded on an IRPrestige-21 Fourier transform infrared spectrophotometer (Shimadzu, Tokyo, Japan). ^{1}H NMR and ^{13}C NMR spectra were recorded on a Varian Mercury 400 FT-NMR spectrometer (Agilent, Palo Alto, CA) operating at 400 and 100 MHz, respectively. Chemical shifts were reported in parts per million (ppm). Tetramethylsilane (TMS) was used

as an internal standard. In the NMR spectra, the splitting patterns were designated as follows: s: singlet; brs: broad singlet; d: doublet; t: triplet; m: multiplet; dd: doublet of doublets. Coupling constants (*J*) were reported in Hertz (Hz). HRMS spectra were recorded on an LCMS-IT-TOF (Shimadzu) using the electrospray ionization (ESI) technique. Thin-layer chromatography (TLC) was performed on TLC Silica gel 60 F_{254} aluminum sheets (Merck) to monitor the progress of the chemical reactions and check the purity of the synthesized compounds.

The InChI codes of the investigated compounds, together with some biological activity data, are provided as Supporting Information.

4.1.2 | Synthesis of 2-chloro-*N*-(2-methylbenzoxazol-5-yl)acetamide (1)

Chloroacetyl chloride (0.1 mol) was added dropwise, with stirring, to a mixture of 5-amino-2-methylbenzoxazole (0.1 mol) and TEA (0.1 mol) in toluene (50 ml) at 0–5°C. Upon completion of the reaction, the solvent was evaporated using Rotavapor® R-100 (Büchi, Switzerland). The residue was washed with water and filtered. After drying, the product was crystallized from ethanol.[42]

4.1.3 | Synthesis of 5-substituted benzoxazole-2-thiol derivatives (2a – d)/5-substituted 1*H*-benzimidazole-2-thiol derivatives (2e – i)

4-Substituted-*o*-aminophenol/4-substituted-*o*-phenylenediamine (20 mmol) and 40 ml of absolute ethanol were added to a 100 ml-round bottom flask, and the content was stirred for 15 min. In the meanwhile, potassium hydroxide pellets (20 mmol) were powdered and transferred into the flask, followed by the addition of carbon disulfide (15 ml). The mixture was refluxed for 8 hr. Upon completion of the reaction, the solvent was evaporated using Rotavapor® R-100 to yield a solid product. This product was carefully transferred into a beaker and 75 ml of water was added. The solution was acidified with acetic acid until a precipitate appeared. The precipitate was filtered and then washed with water and dried. The product was crystallized from ethanol.[43]

4.1.4 | Synthesis of 2-[(5-substituted benzoxazol/benzimidazol-2-yl)thio]-*N*-(2-methylbenzoxazol-5-yl)-acetamide derivatives (3a – i)

Compounds **2a – i** (1.5 mmol) were treated with 2-chloro-*N*-(2-methylbenzoxazol-5-yl)acetamide (**1**) (1.5 mmol) in the presence of potassium carbonate (1.5 mmol) in acetone (25 ml) at room temperature for 12 hr. Upon completion of the reaction, the solvent was evaporated using Rotavapor® R-100. The residue was washed with water and dried. The product was crystallized from ethanol.

*2-[(5-Nitrobenzoxazol-2-yl)thio]-*N*-(2-methylbenzoxazol-5-yl)-acetamide (**3a**)*

Yield: 85%. M.p.: 147.6°C. IR ν_{max} (cm^{-1}): 3,334.92 (N—H stretching), 3,076.46 (aromatic C—H stretching), 2,983.88, 2,929.87 (aliphatic C—H stretching), 1,675.15 (C═O stretching), 1,625.99, 1,573.91, 1,517.98, 1,477.47 (N—H bending, C═N and C═C stretching), 1,435.04, 1,371.39, 1,332.81, 1,257.59, 1,220.94, 1,161.15, 1,116.78, 1,082.07 (C—H bending, C—N, C—O stretching and aromatic C—H in plane bending), 929.69, 893.04, 823.60, 779.24, 748.38, 663.51 (aromatic C—H out of plane bending and C—S stretching). ^{1}H NMR (400 MHz, DMSO-d_6) δ (ppm): 2.64 (s, 3H), 4.20 (s, 2H), 6.94 (d, J = 9.2 Hz, 1H), 7.44 (d, J = 8.0 Hz, 1H), 7.68–7.89 (m, 4H), 10.60 (s, 1H). ^{13}C NMR (100 MHz, DMSO-d_6) δ (ppm): 14.12 (CH_3), 33.05 (CH_2), 110.42 (CH), 116.53 (CH), 117.12 (CH), 119.60 (CH), 121.90 (CH), 125.11 (CH), 131.21 (C), 136.32 (C), 137.97 (C), 141.34 (C), 149.96 (C), 157.83 (C), 158.28 (C), 165.15 (C), 171.87 (C). HRMS (ESI) (*m/z*): $[M + H]^+$ calcd. for $C_{17}H_{12}N_4O_5S$: 385.0601, found: 385.0613.

*2-[(5-Fluorobenzoxazol-2-yl)thio]-*N*-(2-methylbenzoxazol-5-yl)-acetamide (**3b**)*

Yield: 78%. M.p. 142.1°C. IR ν_{max} (cm^{-1}): 3,269.34 (N—H stretching), 3,068.75 (aromatic C—H stretching), 2,978.09, 2,929.87 (aliphatic C—H stretching), 1,675.15 (C═O stretching), 1,633.71, 1,608.63, 1,575.84, 1,477.47 (N—H bending, C═N and C═C stretching), 1,435.04, 1,369.46, 1,253.73, 1,174.65, 1,136.07, 1,091.71 (C—H bending, C—N, C—O stretching and aromatic C—H in plane bending), 962.48, 933.55, 848.68, 808.17, 725.23, 663.51 (aromatic C—H out of plane bending and C—S stretching). ^{1}H NMR (400 MHz, DMSO-d_6) δ (ppm): 2.65 (s, 3H), 4.22 (s, 2H), 6.83–6.87 (m, 1H), 7.36–7.38 (m, 1H), 7.43–7.81 (m, 3H), 8.01 (s, 1H), 10.64 (s, 1H). ^{13}C NMR (100 MHz, DMSO-d_6) δ (ppm): 14.13 (CH_3), 32.93 (CH_2), 108.09 (CH), 109.64 (d, J = 25.2 Hz, CH), 110.38 (CH), 110.60 (CH), 110.67 (CH), 116.49 (CH), 136.44 (C), 141.37 (C), 144.63 (C), 146.70 (C), 149.94 (C), 156.36 (C), 159.66 (C), 165.25 (C), 171.89 (C). HRMS (ESI) (*m/z*): $[M + H]^+$ calcd. for $C_{17}H_{12}FN_3O_3S$: 358.0656, found: 358.0658.

*2-[(5-Chlorobenzoxazol-2-yl)thio]-*N*-(2-methylbenzoxazol-5-yl)-acetamide (**3c**)*

Yield: 84%. M.p. 120.4°C. IR ν_{max} (cm^{-1}): 3,336.85 (N—H stretching), 3,068.75 (aromatic C—H stretching), 2,976.16, 2,929.87 (aliphatic C—H stretching), 1,674.21 (C═O stretching), 1,620.21, 1,597.06, 1,573.91, 1,477.47 (N—H bending, C═N and C═C stretching), 1,435.04, 1,365.60, 1,251.80, 1,172.72, 1,112.93, 1,082.07 (C—H bending, C—N, C—O stretching and aromatic C—H in plane bending), 898.83, 869.90, 808.17, 779.24, 663.51 (aromatic C—H out of plane bending and C – S stretching). ^{1}H NMR (400 MHz, DMSO-d_6) δ (ppm): 2.64 (s, 3H), 4.21 (s, 2H), 6.81–6.87 (m, 2H), 6.96 (d, J = 8.4 Hz, 1H), 7.35–7.44 (m, 1H), 7.74–7.80 (m, 2H), 10.61 (s, 1H). ^{13}C NMR (100 MHz, DMSO-d_6) δ (ppm): 14.13 (CH_3), 32.94 (CH_2), 110.44 (CH), 117.52 (CH), 119.53 (CH), 120.94 (CH), 122.25 (CH), 124.47 (CH), 125.07 (C), 131.22 (C), 136.94 (C), 141.34 (C), 147.27 (C), 149.93 (C), 157.85 (C), 165.19 (C), 171.83 (C). HRMS (ESI) (*m/z*): $[M + H]^+$ calcd. for $C_{17}H_{12}ClN_3O_3S$: 374.0361, found: 374.0363.

*2-[(5-Methylbenzoxazol-2-yl)thio]-N-(2-methylbenzoxazol-5-yl)-acetamide (**3d**)*

Yield: 81%. M.p. 112.9°C. IR ν_{max} (cm^{-1}): 3,321.42 (N—H stretching), 3,068.75 (aromatic C—H stretching), 2,972.31, 2,927.94 (aliphatic C—H stretching), 1,674.21 (C=O stretching), 1,627.92, 1,595.13, 1,577.77, 1,475.54 (N—H bending, C=N and C=C stretching), 1,435.04, 1,357.89, 1,255.66, 1,203.58, 1,176.58, 1,155.36, 1,109.07 (C—H bending, C—N, C—O stretching and aromatic C—H in plane bending), 931.62, 866.04, 831.32, 796.60, 680.87, 661.58 (aromatic C—H out of plane bending and C—S stretching). ^{1}H NMR (400 MHz, DMSO-d_6) δ (ppm): 2.39 (s, 3H), 2.64 (s, 3H), 4.41 (s, 2H), 6.74 (t, J = 8.4 Hz, 1H), 7.42–7.80 (m, 4H), 8.01 (d, J = 1.2 Hz, 1H), 10.60 (s, 1H). ^{13}C NMR (100 MHz, DMSO-d_6) δ (ppm): 14.12 (CH_3), 20.90 (CH_3), 32.81 (CH_2), 109.57 (CH), 110.25 (CH), 116.08 (CH), 116.48 (CH), 118.16 (CH), 125.13 (CH), 134.06 (C), 135.38 (C), 141.34 (C), 145.64 (C), 146.69 (C), 149.90 (C), 156.52 (C), 165.16 (C), 171.89 (C). HRMS (ESI) (*m/z*): $[M + H]^+$ calcd. for $C_{18}H_{15}N_3O_3S$: 354.0907, found: 354.0908.

*2-[(5-Nitro-1H-benzimidazol-2-yl)thio]-N-(2-methylbenzoxazol-5-yl) acetamide (**3e**)*

Yield: 86%. M.p. 263.4°C. IR ν_{max} (cm^{-1}): 3,282.84 (N—H stretching), 3,068.75 (aromatic C—H stretching), 2,962.66, 2,916.37, 2,881.65 (aliphatic C—H stretching), 1,660.71 (C=O stretching), 1,620.21, 1,573.91, 1,537.27, 1,487.12 (N – H bending, C=N and C=C stretching), 1,415.75, 1,381.03, 1,336.67, 1,278.81, 1,244.09, 1,192.01, 1,126.43, 1,064.71 (C—H bending, C—N, C—O stretching and aromatic C—H in plane bending), 966.34, 939.33, 896.90, 871.82, 817.82, 738.74, 690.52, 669.30 (aromatic C – H out of plane bending and C—S stretching). ^{1}H NMR (400 MHz, DMSO-d_6) δ (ppm): 2.60 (s, 3H), 4.42 (s, 2H), 7.47 (dd, J = 1.6 Hz, 8.8 Hz, 1H), 7.61 (t, J = 8.4 Hz, 2H), 8.02 (d, J = 1.6 Hz, 1H), 8.08 (dd, J = 2.4 Hz, 8.8 Hz, 1H), 8.33 (d, J = 2.4 Hz, 1H), 10.61 (s, 1H), 12.56 (brs, 1H). ^{13}C NMR (100 MHz, DMSO-d_6) δ (ppm): 14.10 (CH_3), 36.25 (CH_2), 109.53 (2CH), 110.20 (2CH), 116.39 (CH), 117.49 (CH), 135.44 (C), 141.31 (2C), 142.14 (C), 146.62 (2C), 156.06 (C), 164.69 (C), 165.58 (C). HRMS (ESI) (*m/z*): $[M + H]^+$ calcd. for $C_{17}H_{13}N_5O_4S$: 384.0761, found: 384.0764.

*2-[(5-Fluoro-1H-benzimidazol-2-yl)thio]-N-(2-methylbenzoxazol-5-yl)acetamide (**3f**)*

Yield: 82%. M.p. 234.5°C. IR ν_{max} (cm^{-1}): 3,304.06 (N—H stretching), 3,091.89, 3,064.89 (aromatic C—H stretching), 2,914.44, 2,808.36 (aliphatic C—H stretching), 1,662.64 (C=O stretching), 1,625.99, 1,575.84, 1,537.27, 1,490.97 (N—H bending, C=N and C=C stretching), 1,435.04, 1,408.04, 1,396.46, 1,346.31, 1,311.59, 1,276.88, 1,263.37, 1,195.87, 1,182.36, 1,134.14, 1,103.28 (C—H bending, C—N, C—O stretching and aromatic C—H in plane bending), 939.33, 896.90, 867.97, 817.82, 786.96, 767.67, 721.38, 690.52, 661.58 (aromatic C—H out of plane bending and C—S stretching). ^{1}H NMR (400 MHz, DMSO-d_6) δ (ppm): 2.60 (s, 3H), 4.33 (s, 2H), 7.00 (t, J = 8.8 Hz, 1H), 7.31 (d, J = 8.8 Hz, 1H), 7.46 (d, J = 8.0 Hz, 2H), 7.60 (d, J = 8.4 Hz, 1H), 8.02 (s, 1H), 10.60 (s, 1H), 12.81 (brs, 1H). ^{13}C NMR (100 MHz, DMSO-d_6) δ (ppm): 14.09 (CH_3), 36.28 (CH_2), 109.24 (d, J = 25.2 Hz, CH), 109.56 (2CH), 110.19 (2CH), 116.39 (CH), 135.51 (C), 141.35 (2C), 146.65 (C), 151.31 (C), 157.14 (C), 159.47 (C), 164.68 (C), 166.03 (C). HRMS (ESI) (*m/z*): $[M + H]^+$ calcd. for $C_{17}H_{13}FN_4O_2S$: 357.0816, found: 357.0819.

*2-[(5-Chloro-1H-benzimidazol-2-yl)thio]-N-(2-methylbenzoxazol-5-yl)acetamide (**3g**)*

Yield: 85%. M.p. 239.5°C. IR ν_{max} (cm^{-1}): 3,300.20 (N—H stretching), 3,130.47, 3,062.96 (aromatic C—H stretching), 2,953.02, 2,916.37, 2,881.65 (aliphatic C—H stretching), 1,662.64 (C=O stretching), 1,625.99, 1,573.91, 1,541.12, 1,489.05, 1,456.26 (N—H bending, C=N and C=C stretching), 1,435.04, 1,396.46, 1,348.24, 1,311.59, 1,276.88, 1,195.87, 1,182.36, 1,124.50, 1,058.92 (C—H bending, C—N, C—O stretching and aromatic C—H in plane bending), 964.41, 941.26, 920.05, 896.90, 871.82, 817.82, 786.96, 721.38, 698.23, 661.58 (aromatic C—H out of plane bending and C—S stretching). ^{1}H NMR (400 MHz, DMSO-d_6) δ (ppm): 2.60 (s, 3H), 4.35 (s, 2H), 7.17 (dd, J = 1.6 Hz, 8.4 Hz, 1H), 7.45–7.49 (m, 2H), 7.54 (d, J = 1.2 Hz, 1H), 7.60 (d, J = 8.8 Hz, 1H), 8.03 (d, J = 1.6 Hz, 1H), 10.61 (s, 1H), 12.87 (brs, 1H). ^{13}C NMR (100 MHz, DMSO-d_6) δ (ppm): 14.10 (CH_3), 36.22 (CH_2), 109.51 (CH), 110.20 (2CH), 116.37 (2CH), 121.60 (CH), 125.91 (C), 135.48 (2C), 141.32 (2C), 146.62 (C), 151.74 (C), 164.68 (C), 165.90 (C). HRMS (ESI) (*m/z*): $[M + H]^+$ calcd. for $C_{17}H_{13}ClN_4O_2S$: 373.0521, found: 373.0537.

*2-[(5-Methyl-1H-benzimidazol-2-yl)thio]-N-(2-methylbenzoxazol-5-yl)acetamide (**3h**)*

Yield: 81%. M.p. 204.7°C. IR ν_{max} (cm^{-1}): 3,307.92 (N—H stretching), 3,134.33, 3,061.03, 3,032.10 (aromatic C—H stretching), 2,960.73, 2,914.44 (aliphatic C—H stretching), 1,662.64 (C=O stretching), 1,625.99, 1,577.77, 1,539.20, 1,487.12 (N—H bending, C=N and C=C stretching), 1,436.97, 1,409.96, 1,396.46, 1,381.03, 1,338.60, 1,311.59, 1,276.88, 1,197.79, 1,182.36, 1,124.50 (C—H bending, C—N, C—O stretching and aromatic C—H in plane bending), 968.27, 943.19, 896.90, 873.75, 854.47, 833.25, 817.82, 786.96, 759.95, 721.38, 682.80, 663.51 (aromatic C—H out of plane bending and C—S stretching). ^{1}H NMR (400 MHz, DMSO-d_6) δ (ppm): 2.41 (s, 3H), 2.60 (s, 3H), 4.37 (s, 2H), 6.99 (d, J = 7.6 Hz, 1H), 7.32–7.61 (m, 4H), 8.10 (s, 1H), 10.76 (s, 1H), 12.63 (brs, 1H). ^{13}C NMR (100 MHz, DMSO-d_6) δ (ppm): 14.09 (CH_3), 21.18 (CH_3), 36.35 (CH_2), 109.55 (CH), 110.19 (2CH), 116.36 (2CH), 122.87 (CH), 135.57 (2C), 141.39 (2C), 146.66 (2C), 149.28 (C), 164.65 (C), 166.28 (C). HRMS (ESI) (*m/z*): $[M + H]^+$ calcd. for $C_{18}H_{16}N_4O_2S$: 353.1067, found: 353.1067.

*2-[(5-Methoxy-1H-benzimidazol-2-yl)thio]-N-(2-methylbenzoxazol-5-yl)acetamide (**3i**)*

Yield: 83%. M.p. 177.7°C. IR ν_{max} (cm^{-1}): 3,304.06 (N—H stretching), 3,084.18, 3,001.24 (aromatic C—H stretching), 2,935.66, 2,837.29 (aliphatic C—H stretching), 1,672.28 (C=O stretching), 1,629.85, 1,568.13, 1,481.33 (N—H bending, C=N and C=C stretching), 1,431.18, 1,386.82, 1,355.96, 1,303.88, 1,269.16, 1,203.58, 1,178.51, 1,151.50, 1,111.00, 1,029.99 (C—H bending, C—N, C—O stretching and aromatic C – H in plane bending), 981.77, 929.69, 848.68,

798.53, 765.74, 690.52, 663.51 (aromatic C—H out of plane bending and C—S stretching). ^{1}H NMR (400 MHz, DMSO-d_6) δ (ppm): 2.60 (s, 3H), 3.79 (s, 3H), 4.29 (s, 2H), 6.79 (dd, J = 2.0 Hz, 8.4 Hz, 1H), 7.01 (s, 1H), 7.39 (d, J = 8.8 Hz, 1H), 7.46 (dd, J = 2.0 Hz, 8.8 Hz, 1H), 7.60 (d, J = 8.4 Hz, 1H), 8.03 (d, J = 2.0 Hz, 1H), 10.66 (s, 1H), 12.60 (brs, 1H). ^{13}C NMR (100 MHz, DMSO-d_6) δ (ppm): 14.09 (CH_3), 37.71 (CH_2), 55.46 (CH_3), 104.55 (CH), 109.63 (CH), 110.21 (2CH), 113.61 (CH), 116.47 (CH), 131.76 (C), 135.40 (C), 141.32 (2C), 146.67 (C), 153.84 (C), 158.66 (C), 165.14 (C), 167.02 (C). HRMS (ESI) (m/z): $[M + H]^+$ calcd. for $C_{18}H_{16}N_4O_3S$: 369.1016, found: 369.1022.

4.2 | Biochemistry

4.2.1 | Cell culture and drug treatment

A549 Human lung adenocarcinoma (ATCC® CCL-185™) and NIH/3T3 mouse embryonic fibroblast (ATCC® CRL-1658™) cell lines were cultured and drug treatments were carried out as previously described.[44]

4.2.2 | MTT assay

The level of cellular 3-(4,5-dimethylthiazol-2-yl)−2,5-diphenyltetrazolium bromide (MTT; Sigma-Aldrich, St. Louis, MO) reduction was quantified as previously described in the literature,[45] with small modifications.[44] Compounds **3a** – **i** were investigated for their anticancer activity against the A549 human lung adenocarcinoma cell line. NIH/3T3 mouse embryonic fibroblast cells were used to evaluate the selectivity of the compounds.

After 24 hr of preincubation, compounds **3a** – **i** and cisplatin (positive control) were added to give a final concentration in the range of 1–500 μM and the cells were incubated for 24 hr. At the end of this period, MTT was added to a final concentration of 0.5 mg/ml and the cells were incubated for 4 hr at 37°C. After the medium was removed, the formazan crystals formed by MTT metabolism were solubilized by the addition of 200 μl dimethyl sulfoxide (DMSO) to each well and absorbance was read at 540 nm with a microtiter plate spectrophotometer (Bio-Tek Plate Reader, Winooski, VT). Each concentration was repeated in three wells. The half-maximal inhibitory concentration (IC_{50}) values were defined as the drug concentrations that reduced absorbance to 50% of control values. The SI values were also calculated according to the following formula[46]:

$$SI = IC_{50} \text{ for NIH/3T3 cell line} / IC_{50} \text{ for A549 cellline.}$$

4.2.3 | Flow cytometric analyses of apoptosis

After the incubation of A549 cells with compounds **3e** and **3g** at IC_{50}/2 and IC_{50} concentrations and cisplatin at IC_{50} concentration, phosphatidylserine externalization, which indicates early apoptosis, was detected using FITC Annexin V Apoptosis Detection Kit (BD Pharmingen, San Jose, CA) on a BD FACSAria flow cytometer for 24 hr. Annexin V staining protocol was applied according to the manufacturer's instructions (BD Pharmingen) and analyzed by a BD FACSAria flow cytometer using FACSDiva version 6.1.1 software (BD Biosciences, San Jose, CA).[44]

4.2.4 | SIRT1 activity detection by ELISA

C6 rat glioma cells were administrated by IC_{50} or IC_{50}/2 concentrations of compounds **3e** and **3g** and cisplatin for 24 hr. Cells were detached with trypsin and then collected by centrifugation. After cells were washed by 1× PBS for three times, cell lysates were prepared by frozen cells at ≤−20°C. Freeze/thaw cycles were repeated for three times. Then cells were centrifuged at 1,500*g* for 10 min at 2–8°C to remove cellular debris. Rat Sirtuin-1 activity protocol was applied according to the manufacturer's instructions (USCN, Life Science Inc., Wuhan, China). Briefly, all standards, reagents, and samples were prepared. Also, 100 μl standard or sample was added to each well and incubated for 2 hr at 37°C, and 100 μl detection reagent A was added and incubated for 1 hr at 37°C. Then solutions were aspirated and the wells were washed three times. Then 100 μl detection reagent B was added and incubated for 30 min at 37°C. The solutions were aspirated and washed five times. Then, 90 μl substrate solution was added and incubated for 15–25 min at 37°C. After 50 μl stop solution was added, the plate was read at 450 nm with a microtiter plate spectrophotometer (Bio-Tek plate reader). Each concentration was repeated in double wells. The results were expressed as ng/ml.[44]

4.3 | Statistical analyses

Statistical Package for the Social Sciences (SPSS, Chicago, IL) for Windows 15.0 was used for statistical analysis. Data were expressed as mean ± *SD*. Comparisons were performed by one-way analysis of variance test for normally distributed continuous variables, and post-hoc analyses of group differences were expressed by the Tukey test. The $p < .05$ was considered as statistically significant in this study.

4.4 | Molecular docking studies

Compounds **3e** and **3g** were docked to the active site of SIRT1. Ligands were prepared with energy minimization in ligand preparation program of Schrödinger's Maestro molecular modeling package (Schrödinger Release 2016-2: Schrödinger, LLC, New York, NY) at physiological pH (pH = 7.4) using Optimized Potential Liquid Simulations (OPLS_2005) force field, and the crystal structure of SIRT1 was retrieved from Protein Data Bank server (PDB code: 4IG9) and optimized for docking analysis in protein preparation module of Schrödinger's Maestro molecular modeling package. In molecular docking simulations, Glide/XP docking protocols were applied for the prediction of the topologies of the compounds in the active site of the target structure.[47]

4.5 | In silico ADME studies

The QikProp module of Schrödinger's Molecular modeling package (Schrödinger Release 2016-2, QikProp, Schrödinger) was used to predict the pharmacokinetic profiles of compounds **3a – i**. On the basis of Lipinski's rule of five and Jorgensen's rule of three, all compounds were evaluated for their druglikeness and oral bioavailability.

CONFLICT OF INTERESTS

The authors declare that there are no conflicts of interests.

ORCID

Belgin Sever http://orcid.org/0000-0003-4847-9711
Gülşen Akalın Çiftçi https://orcid.org/0000-0001-5098-8967
Mehlika Dilek Altıntop http://orcid.org/0000-0002-8159-663X

REFERENCES

[1] S. L. Wood, M. Pernemalm, P. A. Crosbie, A. D. Whetton, *Cancer Treat. Rev.* **2015**, *41*, 361.
[2] A. V. Nascimento, H. Bousbaa, D. Ferreira, B. Sarmento, *Curr. Drug Targets* **2015**, *16*, 1448.
[3] L. Li, T. Zhu, Y.-F. Gao, W. Zheng, C.-J. Wang, L. Xiao, M. S. Huang, J. Y. Yin, H. H. Zhou, Z. Q. Liu, *Int. J. Mol. Sci.* **2016**, *17*, 839.
[4] J. Ansari, R. E. Shackelford, H. El-Osta, *Transl. Lung Cancer Res.* **2016**, *5*, 155.
[5] J. Gyoba, S. Shan, W. Roa, E. L. R. Bédard, *Int. J. Mol. Sci.* **2016**, *17*, 494.
[6] Z. Lin, D. Fang, *Genes Cancer* **2013**, *4*, 97.
[7] J. Choupani, S. Mansoori Derakhshan, S. Bayat, M. R. Alivand, M. S. Khaniani, *J. Cell. Physiol.* **2018**, *233*, 4443.
[8] L. Bosch-Presegué, A. Vaquero, *Genes Cancer* **2011**, *2*, 648.
[9] X. Bai, L. Yao, X. Ma, X. Xu, *Mini-Rev. Med. Chem.* **2018**, *18*, 1151.
[10] N. Mautone, C. Zwergel, A. Mai, D. Rotili, *Expert Opin. Ther. Pat.* **2020**, *30*, 389.
[11] H. Karbasforooshan, A. Roohbakhsh, G. Karimi, *Exp. Cell Res.* **2018**, *367*, 1.
[12] B. Padmanabhan, M. Ramu, S. Mathur, S. Unni, S. Thiyagarajan, *Med. Chem.* **2016**, *12*, 347.
[13] J. Hu, H. Jing, H. Lin, *Future Med. Chem.* **2014**, *6*, 945.
[14] A. Gomtsyan, *Chem. Heterocycl. Compd.* **2012**, *48*, 7.
[15] M. Kale, V. Chavan, *Mini-Rev. Org. Chem.* **2019**, *16*, 111.
[16] C. S. Demmer, L. Bunch, *Eur. J. Med. Chem.* **2015**, *97*, 778.
[17] S. Rajasekhar, B. Maiti, K. Chanda, *Synlett* **2017**, *28*, 521.
[18] S. M. Rida, F. A. Ashour, S. A. M. El-Hawash, M. M. ElSemary, M. H. Badr, M. A. Shalaby, *Eur. J. Med. Chem.* **2005**, *40*, 949.
[19] M. A. Abdelgawad, A. Belal, H. A. Omar, L. Hegazy, M. E. Rateb, *Arch. Pharm. Chem. Life Sci.* **2013**, *346*, 534.
[20] Y. An, E. Lee, Y. Yu, J. Yun, M. Y. Lee, J. S. Kang, W.-Y. Kim, R. Jeon, *Bioorg. Med. Chem. Lett.* **2016**, *26*, 3067.
[21] M. A. Abdelgawad, R. B. Bakr, H. A. Omar, *Bioorg. Chem.* **2017**, *74*, 82.
[22] A. Belal, M. A. Abdelgawad, *Res. Chem. Intermed.* **2017**, *43*, 3859.
[23] T. Taskin, S. Yilmaz, I. Yildiz, I. Yalcin, E. Aki, *SAR QSAR Environ. Res.* **2012**, *23*, 345.
[24] S. Yaghmaei, P. Ghalayania, S. Salami, F. Nourmohammadian, S. Koohestanimobarhan, V. Imeni, *Anti-Cancer Agents Med. Chem.* **2017**, *17*, 608.
[25] A.-M. M. E. Omar, O. M. AboulWafa, M. S. El-Shoukrofy, M. E. Amr, *Bioorg. Chem.* **2020**, *96*, 103593.
[26] L. Garuti, M. Roberti, G. Bottegoni, *Curr. Med. Chem.* **2014**, *21*, 2284.
[27] F. Fei, Z. Zhou, *Expert Opin. Ther. Pat.* **2013**, *23*, 1157.
[28] P. Singla, V. Luxami, K. Paul, *RSC Adv.* **2014**, *4*, 12422.
[29] O. O. Ajani, D. V. Aderohunmu, C. O. Ikpo, A. E. Adedapo, I. O. Olanrewaju, *Arch. Pharm. Chem. Life Sci.* **2016**, *349*, 475.
[30] G. Yadav, S. Ganguly, *Eur. J. Med. Chem.* **2015**, *97*, 419.
[31] W. Akhtar, M. F. Khan, G. Verma, M. Shaquiquzzaman, M. A. Rizvi, S. H. Mehdi, M. Akhter, M. M. Alam, *Eur. J. Med. Chem.* **2017**, *126*, 705.
[32] C. Karaaslan, Y. Duydu, A. Ustundag, C. O. Yalcin, B. Kaskatepe, H. Goker, *Med. Chem.* **2019**, *15*, 287.
[33] Y. K. Yoon, M. A. Ali, A. C. Wei, A. N. Shirazi, K. Parang, T. S. Choon, *Eur. J. Med. Chem.* **2014**, *83*, 448.
[34] Y. K. Yoon, M. A. Ali, A. C. Wei, T. S. Choon, H. Osman, K. Parang, A. N. Shirazi, *Bioorg. Med. Chem.* **2014**, *22*, 703.
[35] Y. K. Yoon, H. Osman, T. S. Choon, *Med. Chem. Commun.* **2016**, *7*, 2094.
[36] M. O. Radwan, D. Takaya, R. Koga, K. Iwamaru, H. Tateishi, T. F. S. Ali, A. Takaori-Kondo, M. Otsuka, T. Honma, M. Fujita, *Bioorg. Med. Chem.* **2020**, *28*, 115409.
[37] R. S. Y. Wong, *J. Exp. Clin. Cancer Res.* **2011**, *30*, 87.
[38] A. El-Khattouti, D. Selimovic, Y. Haikel, M. Hassan, *J. Cell Death* **2013**, *6*, 37.
[39] A. Kamal, S. Faazil, M. S. Malik, *Expert Opin. Ther. Pat.* **2014**, *24*, 339.
[40] R. M. Mohammad, I. Muqbil, L. Lowe, C. Yedjou, H.-Y. Hsu, L.-T. Lin, M. D. Siegelin, C. Fimognari, N. B. Kumar, Q. P. Dou, H. Yang, A. K. Samadi, G. L. Russo, C. Spagnuolo, S. K. Ray, M. Chakrabarti, J. D. Morre, H. M. Coley, K. Honoki, H. Fujii, A. G. Georgakilas, A. Amedei, E. Niccolai, A. Amin, S. S. Ashraf, W. G. Helferich, X. Yang, C. S. Boosani, G. Guha, D. Bhakta, M. R. Ciriolo, K. Aquilano, S. Chen, S. I. Mohammed, W. N. Keith, A. Bilsland, D. Halicka, S. Nowsheen, A. S. Azmi, *Semin. Cancer Biol.* **2015**, *35*, S78.
[41] M. M. Pore, T. J. N. Hiltermann, F. A. E. Kruyt, *Cancer Lett.* **2013**, *332*, 359.
[42] M. D. Altintop, Z. A. Kaplancikli, G. Turan-Zitouni, A. Özdemir, F. Demirci, G. Iscan, G. Revial, *Synth. Commun.* **2011**, *41*, 2234.
[43] T. K. Venkatachalam, G. K. Pierens, D. C. Reutens, *Lett. Org. Chem.* **2010**, *7*, 519.
[44] M. D. Altıntop, H. E. Temel, B. Sever, G. Akalın Çiftçi, Z. A. Kaplancıklı, *Molecules* **2016**, *21*, 1598.
[45] T. Mosmann, *J. Immunol. Methods* **1983**, *65*, 55.
[46] H.-Y. Zhou, F.-Q. Dong, X.-L. Du, Z.-K. Zhou, H.-R. Huo, W.-H. Wang, H. D. Zhan, Y. F. Dai, Jing Meng, Y. P. Sui, J. Li, F. Sui, Y. H. Zhai, *Bioorg. Med. Chem. Lett.* **2016**, *26*, 3876.
[47] A. M. Davenport, F. M. Huber, A. Hoelz, *J. Mol. Biol.* **2014**, *426*, 526.

SUPPORTING INFORMATION

Additional supporting information may be found online in the Supporting Information section.

How to cite this article: Sever B, Akalın Çiftçi G, Altıntop MD. A new series of benzoxazole-based SIRT1 modulators for targeted therapy of non-small-cell lung cancer. *Arch Pharm.* 2021;354:e2000235. https://doi.org/10.1002/ardp.202000235